

Article

# Vector Meson Spectrum from Top-Down Holographic QCD

Mohammed Mia<sup>1</sup>, Keshav Dasgupta<sup>2,\*</sup> , Charles Gale<sup>2</sup>, Michael Richard<sup>2</sup> and Olivier Trottier<sup>2</sup>

<sup>1</sup> Department of Physics and Astronomy, Purdue University, 525 Northwestern Avenue, West Lafayette, IN 47907, USA; mmia@purdue.edu

<sup>2</sup> Department of Physics, McGill University, 3600 University Street, Montreal, QC H3A 2T8, Canada; gale@physics.mcgill.ca (C.G.)

\* Correspondence: keshav@hep.physics.mcgill.ca

**Abstract:** We elaborate on the brane configuration that gives rise to a QCD-like gauge theory that confines at low energies and becomes scale invariant at the highest energies. In the limit where the rank of the gauge group is large, a gravitational description emerges. For the confined phase, we obtain a vector meson spectrum and demonstrate how a certain choice of parameters can lead to quantitative agreement with empirical data.

**Keywords:** high energy physics; supergravity; quantum chromodynamics

**MSC:** 81T28; 81T30; 83E30; 83E50

## 1. Introduction

Quantum Chromo-Dynamics (QCD) is the accepted gauge theory of the strong interaction, and its degrees of freedom are the fermionic quarks (and anti-quarks) and the bosonic gluons. The fact that the gluon gauge fields admit self-interaction creates a scale-dependent coupling: at short distances, smaller than that of a proton, a quark-antiquark pair experiences a Coulomb-like potential while at larger distances the pair binds in a field configuration that is like that of a flux tube. In the regime where the coupling between partons becomes large, calculations of the low-energy properties of QCD have traditionally relied either on large numerical simulation of the theory, discretised on a space-time lattice (“lattice QCD”), or on the use of effective theories based on some of the fundamental symmetries of QCD. However, a new class of approaches that have generated great interest is that based on the concept of holographic duality as expressed through the famous AdS/CFT correspondence [1]. A powerful feature of such dualities is that even though the field theory sector might be strongly coupled, its gravity dual can be treated in perturbation theory. This opens the tantalising prospect of being able to treat systems interacting through low-energy QCD analytically, at least to some extent. Theories that attempt to realise this potential are globally labelled AdS/QCD. Even though no formal gravity dual of QCD is known, several models use holographic techniques to arrive at “QCD-like” field theories, at least to explain the infra-red (IR) dynamics. One important example being the Klebanov–Strassler model [2]. Bottom-up approaches are phenomenologically based and are not as such compelled by the rules of string theory. Top-down approaches start with gauge theory arising from open strings ending on branes and then study the dual closed string sector described by classical gravity. Such an approach, that in fact covers the regime from low to high energies, is used in this work; the next section describes this top-down model. Then, we construct a pseudo-QCD action from our gravity dual, and calculate the vector meson mass spectrum. We compare our results with those obtained using the



Academic Editor: Angel Ricardo Plastino

Received: 27 November 2024

Revised: 14 January 2025

Accepted: 15 January 2025

Published: 16 January 2025

**Citation:** Mia, M.; Dasgupta, K.; Gale, C.; Richard, M.; Trottier, O. Vector Meson Spectrum from Top-Down Holographic QCD. *Axioms* **2025**, *14*, 66. <https://doi.org/10.3390/axioms14010066>

**Copyright:** © 2025 by the authors. Licensee MDPI, Basel, Switzerland. This article is an open access article distributed under the terms and conditions of the Creative Commons Attribution (CC BY) license (<https://creativecommons.org/licenses/by/4.0/>).

Sakai–Sugimoto model, and also with experimentally measured masses. We end with a conclusion.

## 2. Brane Configuration

We start with coincident  $N$  Dirichlet three-branes ( $D3$  branes) and  $M$  Dirichlet five-branes ( $D5$  branes) at the tip of a cone [see Figure 1] and add  $M$  anti-five branes separated from each other and from the  $D3/D5$  branes [see Figure 1]. To obtain this separation, we must blow up one of the  $S^2$ 's at the tip and give it a finite size. The separation gives masses  $\Lambda_0$  to the  $D5/\bar{D}5$  strings and at scales  $\Lambda < \Lambda_0$ , the gauge group is  $SU(N + M) \times SU(N) \times U(1)^M$ , where the additional  $U(1)$  groups arise from the massless strings ending on the  $\bar{D}5$ -branes spread above the equator of the  $S^2$ . The  $SU(M + N)$  sector has  $2N$  effective flavors while the  $SU(N)$  sector has  $2(N + M)$  effective flavors; thus, it is dual to the  $SU(N - M) \times SU(N)$  gauge theory under a Seiberg duality. Under a series of such dualities, which is called cascading, at the far IR region, the gauge theory can be described by an  $SU(M) \times SU(K)$  group, where  $N = lM + K$ ,  $l, 0 \leq K < M$  are positive integers. Now, the number of 'actual'  $D3$  branes  $N$  is no longer the relevant quantity, rather  $N \pm pM$ , where  $p$  is an integer that describes the  $D3$  brane charge. We take  $K = 0$  in all our analysis, so at the bottom of the cascade, we are left with  $\mathcal{N} = 1$  SUSY  $SU(M)$  strongly coupled gauge theory which looks very much like strongly coupled SUSY QCD.

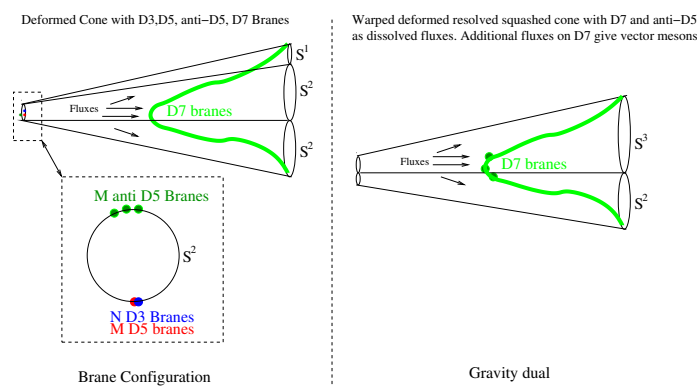


**Figure 1.** Brane configuration and the dual gravity in the extremal limit for a UV regular theory. The anti-branes should be thought of as spread above the equator of the resolved sphere although the branes are all localised at the south pole of the sphere. The manifolds appearing on both sides of the duality are in general non-Kähler manifolds although in the limit of vanishing resolution and squashing they become Kähler Calabi–Yau spaces.

At high energies  $\Lambda \gg \Lambda_0$ ,  $D5/\bar{D}5$  strings are excited and we have  $SU(N + M) \times SU(N + M)$  gauge theory. Essentially,  $M$  pairs of  $D5/\bar{D}5$  branes with fluxes are equivalent to  $M$  number of  $D3$  branes and hence they contribute an additional  $M$  units of  $D3$  charge, resulting in  $SU(N + M) \times SU(N + M)$  conformal theory. In summary, for  $\Lambda \ll \Lambda_0$ , i.e., at low energy, we have an  $SU(M)$  gauge group that confines, while at high energy  $\Lambda \gg \Lambda_0$ , we have a conformal field theory with two copies of the  $SU(N + M)$  group. Pure glue QCD, with a large number of colors, confines in the IR and becomes conformal at the UV; thus, the brane setup gives rise to a QCD-like gauge theory. To add flavor, we can add  $D7$  branes but the overall setup does not change—we still have UV conformal gauge theory that confines in the IR. In fact, the walking RG flow in the UV due to the flavor seven-branes match up precisely with the IR RG flow leading to confinement.

Now, of course, the presence of anti-branes will create tachyonic modes and the system will be unstable. To stabilise the system against gravitational and RR forces, we need to add world volume fluxes on the  $D5/\bar{D}5$  branes. Alternatively, we can introduce  $D7$  branes and absorb the anti- $D5$  branes as gauge fluxes on the  $D7$  branes. Then, a stable configuration of

*D7* branes with gauge fluxes in the presence of coincident *D3/D5* branes will be equivalent to a stable configuration of coincident *D3/D5* branes and anti-*D5* along with *D7* branes. More details on the stabilisation procedure are discussed in [3].

Observe that *D7* branes also introduce fundamental matter and with world volume fluxes on Minkowski directions, they give rise to vector mesons as we shall see shortly. In summary, *D7* branes play two crucial roles: they source the anti-*D5* charge and produce vector mesons for the four-dimensional gauge theory. In principal, different embeddings can be used for distinct purposes. In Figure 1, we have sketched a generic *D7* embedding. Introducing various fluxes will determine the precise embedding and, in turn, modify the gauge theory.

### 3. Gravity Description

When the 'tHooft coupling for the gauge theory is large, which can be achieved, for example, with large *M*, we can obtain a classical gravitational description for the gauge theory arising from the above brane setup. The gravity action arises from the low energy limit of type IIB critical superstring action with localised sources given as:

$$\begin{aligned}
 S_{\text{total}} &= S_{\text{SUGRA}} + N_f S_{Dp} \\
 S_{\text{SUGRA}} &= \frac{1}{2\kappa_{10}^2} \int d^{10}x \sqrt{G} \left( R + \frac{\partial_M \tau \partial^M \bar{\tau}}{2|\text{Im}\tau|^2} - \frac{|\tilde{F}_5|^2}{4 \cdot 5!} \right. \\
 &\quad \left. - \frac{G_3 \cdot \bar{G}_3}{12\text{Im}\tau} \right) + \frac{1}{8i\kappa_{10}^2} \int \frac{C_4 \wedge G_3 \wedge \bar{G}_3}{\text{Im}\tau} \\
 S_{Dp} &= - \int d^{p+1}\sigma T_p e^{\frac{\phi(p+1)}{4}} \sqrt{-f} \left( 1 + e^{-\phi} \frac{1}{4} \tilde{F}^{ab} \tilde{F}_{ab} \right) \\
 &\quad + \mu_p \int (C \wedge e^{\tilde{F}})_{p+1} \tag{1}
 \end{aligned}$$

where  $N_f$  is number of *Dp* branes,  $\tau = C_0 + ie^{-\phi}$ ,  $F_1 = dC_0$  and  $G = \text{det}g_{PQ}$ ,  $P, Q = 0, \dots, 9$  with  $g_{PQ}$  is the metric in the Einstein frame. Also  $G_3 = F_3 - \tau H_3$ ,  $f = \text{det}f_{ab}$  with  $f_{ab} = g_{PQ} \partial_a X^P \partial_b X^Q$ . Note that  $\tilde{F}_{ab} = F_{ab} + B_{ab}$ ,  $F_{ab}$  is the world volume flux,  $B_{ab} = B_{PQ} \partial_a X^P \partial_b X^Q$  with  $B_{PQ}$  being the NS-NS two form and  $\tilde{F}_{ab}$  is raised or lowered with the pullback metric  $f_{ab}$ . The background warped metric takes the following familiar form

$$\begin{aligned}
 ds^2 &= g_{PQ} dx^P dx^Q \equiv g_{\mu\nu} dx^\mu dx^\nu + g_{mn} dx^m dx^n \\
 &= -e^{2A+2B} dt^2 + e^{2A} d\vec{x}^2 + e^{-2A-2B} \tilde{g}_{mn} dx^m dx^n \tag{2}
 \end{aligned}$$

where  $d\vec{x}^2 = dx^2 + dy^2 + dz^2$ ,  $\mu, \nu = 0, \dots, 3, m, n = 4, \dots, 9$  and the internal unwarped metric is given by  $\tilde{g}_{mn} \equiv \tilde{g}_{mn}^0 + \tilde{g}_{mn}^1$ . Here,  $\tilde{g}_{mn}^0$  describes the base of a deformed cone with or without resolution or squashing, while  $\tilde{g}_{mn}^1$  is the perturbation due to the presence of fluxes and localised sources (The resolved deformed cones, with or without squashing, are not Calabi-Yau manifolds but more general non-Kähler manifolds.). A resolved-deformed cone refers to the base where cycles never go to zero size and squashing describes the deviation of shapes from an ordinary *n*-sphere. The resolution, deformation and squashing parameters are a dual description of a particular expectation value of the gauge-invariant combinations of bifundamental matter fields at the far IR of the gauge theory. The right figure in Figure 1 is a sketch of a warped resolved-deformed and squashed conifold which captures the most general dual gravity corresponding to a confining gauge theory with some expectation value of baryonic operators. When resolution and squashing are set to zero, we also have non-zero expectation values, provided we consider a deformed cone

just like Klebanov–Strassler [2]. When we are away from the resolved-deformed tip of the cone and there is no squashing,  $\tilde{g}_{mn}^0$  is the metric of  $R^1 \times T^{1,1}$ .

The action (1) in the absence of any localised sources can describe the gauge theory arising from the brane setup of Figure 1, provided  $G_3 \neq 0$ . When  $G_3 = 0$ , one can obtain an  $AdS_5 \times T^{1,1}$  geometry which describes a CFT [4]. The presence of localised sources allows us to patch together a warped deformed conifold geometry with  $G_3 \neq 0$  at small radial distances to an asymptotically  $AdS_5 \times T^{1,1}$  geometry. The localised sources have to alter  $G_3$ , so we look for  $D5$  or anti- $D5$  branes. We can also dissolve these branes as gauge fluxes on  $D7$  branes. We take the latter approach since it is easier to find stable  $D7$  brane embeddings.

The  $D7$  branes fill up Minkowski space  $(t, x, y, z)$ , stretching along the radial  $r$  direction and filling up  $S^3$  inside the  $T^{1,1} = S^3 \times S^2$ . In the absence of resolution and squashing, ref. [5] proposed  $D7$  branes embeddings that source the world volume fluxes  $\tilde{F}_2$ , inducing the anti- $D5$  charge. There were two branches of the  $D7$  brane and the world volume flux on each branch modifies the background RR and NS-NS three-form flux, resulting in the following fluxes

$$\begin{aligned} F_3 &= \frac{M\alpha'}{2}\omega_3 + 4\kappa_{10}^2\tilde{M}N_f\alpha'\mu_7\left(F(r)\tilde{\omega}_3^1 + H(r)\tilde{\omega}_3^2\right) \\ H_3 &= \frac{*_6(e^B F_3)}{\text{Im}\tau} \end{aligned} \tag{3}$$

where  $*_6$  is the hodge star for the metric  $g_{mn}$ . The definitions of the three forms  $\omega_3, \tilde{\omega}_3^1, \tilde{\omega}_3^2$  and of the scalar functions  $F(r), H(r)$  can be found in [5] (see also earlier works [6–8]). The effective number of  $D5$  branes in the dual gauge theory can be obtained using Gauss’ law:

$$M_{\text{eff}}^{\text{total}} = \int F_3 \tag{4}$$

For a given value of  $M$ , we can choose  $\tilde{M}$  such that

$$\int_{r \rightarrow \infty} F_3 = 0 \Rightarrow M_{\text{eff}}^{\text{total}}(r \rightarrow \infty) = 0 \tag{5}$$

Since the radial coordinate  $r$  is dual to the energy scale of the gauge theory, we find that the total  $D5$  brane charge vanishes in the far UV and we are left only with  $D3$  branes. Thus, for  $r < r_0$ , that is  $\Lambda < \Lambda_0$ , one finds using (3) that  $M_{\text{eff}}^{\text{total}}(\Lambda < \Lambda_0) \sim M$ , i.e., we have  $M$  units of  $D5$  charge.

The introduction of  $r_0$  gives rise to a scale and we divide the geometry into three regions—a classification that will be particularly useful in studying the meson spectrum—Region I:  $r < r_0$ ; Region II:  $r \sim r_0$ ; Region III:  $r \gg r_0$

### 3.1. Confinement and Meson Spectrum

The form of the metric (2) describes a manifold  $X$  with or without a black hole. When  $B = 0$ , we have a geometry without a black hole, while in the presence of a black hole, we have a horizon with radial location  $r = r_h$  such that  $e^{B(r_h)} = 0, e^{2A(r_h)} \neq 0$ . The temperature of the gauge theory dual to  $X$  is determined by the singularity structure of  $X$  in the following way: analytically continue  $\tilde{\tau} = -it$  to obtain the Euclidean metric where  $\tilde{\tau} \in [0, \beta]$ . Then, the temperature is given by  $T^{-1} = \beta$ . In the presence of a black hole,  $X$  is singular and removing the singularity fixes the period  $\beta$ . Thus, for a black hole geometry, the temperature is related to the horizon. On the other hand, in the absence of a black hole, we pick any value of  $\beta$  since we consider warp factors  $e^{-4A} = h$  to be regular on  $X$ . If we denote the ‘vacuum’ geometry without a black hole by  $X^1$  with on-shell action  $\mathcal{S}^1$  and black hole geometry by  $X^2$  with on-shell action  $\mathcal{S}^2$ , then at a given temperature, the geometry

with a smaller value of the on-shell action will be preferred. At  $T = T_c$ ,  $\Delta S \equiv S^2 - S^1 = 0$  and we have a phase transition. At  $T < T_c$ ,  $\Delta S > 0$  and  $X^1$  is preferred [5,9–11]. Since there is no black hole,  $X^1$  corresponds to zero entropy and confinement. On the other hand, for  $T > T_c$ ,  $\Delta S < 0$  and black hole geometry is preferred. Since the black hole has non-zero entropy, the gauge theory is in the deconfined phase and  $T = T_c$  corresponds to the confinement/deconfinement transition temperature.

Thus, at small temperatures  $T < T_c$ , we can consider the ‘vacuum’ geometry without a black hole since it describes the confined phase. We can obtain the meson spectrum by introducing additional  $D7$  branes embedded as probes in the geometry with metric (2) in the limit  $B = 0$ . Note that these probe  $D7$  branes differ from the  $D7$  branes considered in [5]. The additional probe branes with world volume fluxes in Minkowski directions give rise to QCD-like vector mesons. The world volume fluxes on the background  $D7$  branes have no legs in the Minkowski directions and they represent dissolved anti- $D5$  branes necessary for a UV complete theory.

Before going into the details of the probe brane embedding, observe that the energy scale  $\Lambda_0$  corresponding to  $r_0$  provides us a notion of UV and IR energies. Since mesons appear at low energies, we expect the spectrum to be sensitive to Region I with  $r < r_0$  and the characteristic mass scale for the mesons to be set by  $r_c < r_0$ . This mass scale manifests itself in the dual geometry via  $D7$  embedding that stretches from  $r = \infty$  to  $r = r_c$ . Now, if we consider the trivial embedding where the pull back metric is the spacetime metric and the brane is a point in the transverse directions with the embedding function being constant, then the brane will slide down to the region  $r < r_c$  due to gravitational pull. If we consider the brane to have some shape, i.e., the embedding function is not a constant, then it will be possible for it to end at  $r_c$ , just like the U-shaped embedding in [12]. However, the spectrum analysis becomes quite involved for a non-trivial embedding, since the gauge fluxes and embedding will be coupled.

One alternative to avoid such complications is to cut off the geometry at  $r = r_c$  and only consider the  $r \geq r_c$  region. In this scenario, the constant embedding  $D7$  brane will extend from  $r = \infty$  to  $r = r_c$  and  $r_c$  will provide the characteristic scale of the mesons. For instance, all the meson masses will be expressed in units of  $r_c$ . In the following analysis, we will introduce  $r_c$  as a cutoff in the geometry, which essentially acts as an IR cutoff in the gauge theory. The cutoff geometry will have the same form (1) as its action with the boundary condition for metric and fluxes at  $r = r_c$  consistent with the bulk solution without the cutoff.

To draw a parallel with the celebrated Sakai–Sugimoto model [13,14], we T-dualise the metric (2) along the  $\psi$  coordinate of the conifold geometry and analyse the DBI action of a single  $D6$  brane. We pick world volume parametrisation  $(\sigma^0, \dots, \sigma^6) = (t, x, y, z, r, \phi_2, \theta_2)$  and the brane is a point inside  $S^3$  with the embedding:  $(\theta_1, \phi_1, \psi) = (0, 0, \psi(r))$ . The induced metric and  $B$ -field on the  $D6$  world volume are:

$$\begin{aligned}
 f_{ab}dX^a dX^b &= \frac{\eta_{\mu\nu}dx^\mu dx^\nu}{\sqrt{h(r)}} + \frac{9L^4}{r^2\sqrt{h(r)}}\psi'(r)^2 dr^2 \\
 &\quad + \sqrt{h(r)}\left[dr^2 + r^2\left(d\theta_2^2 + (u + \sin(\theta_2)^2)d\phi_2^2\right)\right] \\
 B_2 &= 3g_s M \log(r/r_c) \sin(\theta_2) d\theta_2 \wedge d\phi_2 \\
 &\quad + 2L^2\psi'(r) \cos(\theta_2) dr \wedge d\phi_2 \\
 e^{-\phi(r)} &= \frac{h(r)^{\frac{1}{4}}r}{6g_s}, \quad h(r) = \frac{L^4\left(1 + \frac{3g_s M^2 \log(r/r_c)}{2\pi N}\right)}{4r^4}
 \end{aligned}
 \tag{6}$$

where  $L^4 = 27\pi N\alpha'^2$  and  $u$  is a *squashing* parameter describing a squashed sphere at the base of the cone. Since we will only consider  $u \ll 1$ , we do not show its dependence on the RR fields; and  $(B_2, \phi)$  are kept independent of  $u$ . Also, note that the warp factor  $h(r)$  above is only valid for Region I and we are considering a region away from the resolved/deformed base. Thus, essentially, we consider the T-dual of the warped squashed  $T^{1,1}$ . Solving the embedding equation for  $\psi(r)$ , one finds that  $\psi(r) = c$  (constant) is a solution [3]. For the study of the meson spectrum, one needs to study fluctuations of embedding for which the more convenient coordinates are  $(Y, Z)$ :

$$\begin{aligned} Y &= \rho \cos(\theta), & Z &= \rho \sin(\theta) \\ \rho &= \sqrt{Y^2 + Z^2}, & \theta &= \arctan\left(\frac{Z}{Y}\right) \\ r &= r_c e^\rho, & \psi &= \frac{2c}{\pi} \theta \end{aligned} \tag{7}$$

In this new coordinate system, the constant embedding is described by  $Y = 0$ . Also note that the coordinate transformation makes the IR cutoff  $r = r_c$  manifest since the new coordinate  $\rho \geq 0$  spans the entire cutoff geometry. Finally, if  $r_c$  is bigger than the deformation parameter that appears in Klebanov–Strassler theory (The deformed conifold is characterized by non-zero size of  $S^3$  at base of the conifold, which in turn determines the scale of confinement. The size corresponds to expectation values of gauge invariant combinations of bifundamental fields and gives a length scale. If  $r_c$  is bigger than this length scale, then the cutoff geometry can be identified with  $r > r_c$  regions of deformed cone.), we effectively consider mesons heavier than the confinement scale.

### 3.1.1. Vector Mesons Action

The vector mesons arise by considering the gauge flux ( $A_M$ ) along the Minkowski  $(t, x, y, z)$ - and  $Z$ -directions.

$$\begin{aligned} A_M &= \begin{cases} A_\mu(x^\mu, Z) & \text{when } M = \mu \in \{t, x, y, z\} \\ A_Z(x^\mu, Z) & \text{when } M = Z \\ 0 & \text{when } M \in \{\theta_2, \phi_2\} \end{cases} \\ F_{MN} &= \partial_M A_N - \partial_N A_M \end{aligned} \tag{8}$$

Looking at the terms quadratic in  $F_{MN}$  in the DBI action, we have:

$$\begin{aligned} S_{D6} &= -T \int d^4x dZ d\theta_2 d\phi_2 e^{-\phi(r(0,Z))} \sqrt{-\det(g_6 + \mathcal{B}_6)} \\ &= -(2\pi\alpha')^2 T \int d^4x dZ \left( v_1(Z) \eta^{\mu\nu} F_{\mu Z} F_{\nu Z} \right. \\ &\quad \left. + v_2(Z) \eta^{\mu\nu} \eta^{\rho\sigma} F_{\mu\rho} F_{\nu\sigma} + \dots \right) \end{aligned} \tag{9}$$

where  $\mathcal{B}_6 \equiv B_6 + 2\pi\alpha'$ ; and  $v_1(Z)$  and  $v_2(Z)$  are even functions of  $Z$ , which also have non-trivial dependence on  $u, g_s$  and  $M$ . The algebraic expressions of these functions can be found in [3].

We now expand  $A_\mu$  and  $A_Z$  in eigenmodes using two sets of eigenfunctions  $\{\alpha_n(Z), n \geq 1\}$  and  $\{\beta_n(Z), n \geq 0\}$

$$\begin{aligned} A_\mu(x^\mu, Z) &= \sum_{n=1}^{\infty} B_\mu^{(n)}(x^\mu) \alpha_n(Z) \\ A_Z(x^\mu, Z) &= \sum_{n=0}^{\infty} \varphi^{(n)}(x^\mu) \beta_n(Z) \end{aligned} \tag{10}$$

Focusing on terms proportional to  $\alpha_n^2$ , we obtain terms reminiscent of the vector mesons terms of QCD.

$$\begin{aligned} S_{\alpha_n^2} &= -(2\pi\alpha')^2 T \int d^4x dZ \sum_{m,n} [v_2(Z) F_{\mu\nu}^{(n)} F^{\mu\nu(m)} \alpha_n \alpha_m \\ &\quad + v_1(Z) B_\mu^{(m)} B^{\mu(n)} \dot{\alpha}_m \dot{\alpha}_n] \end{aligned} \tag{11}$$

We will now impose the following conditions on  $\alpha_n$ ,

$$-\partial_Z(v_1(Z) \partial_Z \alpha_n) = 2v_2(Z) m_n^2 \alpha_n \tag{12}$$

$$(2\pi\alpha')^2 T \int dZ v_2(Z) \alpha_m \alpha_n = \frac{1}{4} \delta_{mn} \tag{13}$$

where  $m_n^2 \equiv \lambda_n \mathcal{M}^2$  is the effective squared-mass of each vector meson and  $\lambda_n$  is the eigenvalue of the corresponding mode. As expected, the mass scale  $\mathcal{M}^2$  is given by  $\frac{r_c^2}{4\pi N \alpha'^2}$ . From the last two equations, we can derive the following identity:

$$(2\pi\alpha')^2 T \int dZ v_1(Z) \dot{\alpha}_m \dot{\alpha}_n = \frac{1}{2} m_n^2 \delta_{mn} \tag{14}$$

Using the above relation, the action (11) takes the form resembling QCD.

$$S_{QCD} = - \sum_{n=1}^{\infty} \int d^4x \left( \frac{1}{4} F_{\mu\nu}^{(n)} F^{\mu\nu(n)} + \frac{1}{2} m_n^2 B_\mu^{(n)} B^{\mu(n)} \right) \tag{15}$$

and thus  $m_n$  can indeed be identified with the vector meson mass.

### 3.1.2. Vector Mesons Spectrum

We now solve the eigenvalue Equation (12) by using simple perturbation techniques with  $\delta \equiv \frac{g_s \mathcal{M}^2}{N}$  as the controlling parameter. We introduce some notation to write the problem in terms of a differential operator  $\mathbf{H}_v$  acting on its eigenfunctions  $\alpha_n$  [3].

$$\begin{aligned} (12) &\rightarrow \mathbf{H}_v |\alpha_n\rangle = \lambda_n |\alpha_n\rangle \\ \mathbf{H}_v &\equiv -\frac{v_1(Z)}{2\mathcal{M}^2 v_2(Z)} \left( \partial_Z^2 + \frac{v_1'(Z)}{v_1(Z)} \partial_Z \right) \\ f(Z) &\equiv 4(2\pi\alpha')^2 T v_2(Z) \\ \langle \alpha_m | \alpha_n \rangle &\equiv \int_{\mathbb{R} \setminus \{0\}} dZ f(Z) \alpha_m \alpha_n = \delta_{mn} \end{aligned} \tag{16}$$

We can now solve Equation (16) up to the first order in  $\delta$  obtaining the eigenfunctions and eigenvalues [3]. We impose that the eigenfunctions be normalisable so that the orthog-

onality condition in (16) is satisfied. At zeroth order in  $\delta$ , the eigenfunctions are given in terms of Bessel’s functions of the first kind.

$$\alpha_n^{(0)}(Z) = C e^{-|Z|} J_1\left(\sqrt{\lambda_n} e^{-|Z|}\right) \tag{17}$$

$C$  is determined by using the zeroth-order normalisation condition. The eigenvalues are obtained by solving the following equations, which we expect for odd and even functions. These conditions also guarantee perfect orthonormality of the eigenfunctions:

$$\alpha_n^{(0)}(0, \lambda_n) = 0 \quad (\text{Odd functions}) \tag{18}$$

$$\partial_Z \alpha_n^{(0)}(0, \lambda_n) = 0 \quad (\text{Even functions}) \tag{19}$$

For odd functions, we also add an extra  $\text{sgn}(Z)$  to make them truly odd. Using the same indexing as Sakai and Sugimoto, the eigenfunctions are summarised as follows:

$$\alpha_{2n+1}^{(0)}(Z) = C e^{-|Z|} J_1\left(\sqrt{\lambda_{2n+1}} e^{-|Z|}\right) \tag{20}$$

$$\alpha_{2n}^{(0)}(Z) = C \text{sgn}(Z) e^{-|Z|} J_1\left(\sqrt{\lambda_{2n}} e^{-|Z|}\right) \tag{21}$$

Now, the first-order correction to the eigenvalues of Equation (16) is given by the well-known formula in perturbation theory and is expressed here as [3]:

$$\begin{aligned} \lambda_n^{(1)} &= \langle \alpha_n^{(0)} | \mathbf{H}_v^{(1)} | \alpha_n^{(0)} \rangle^{(0)} \\ \mathbf{H}_v^{(1)} &= \frac{3 e^{2|Z|}}{2\pi} \left[ |Z| \partial_Z^2 - 2 Z \mathcal{G}(u) \partial_Z \right] \\ \mathcal{G}(u) &\equiv 7 - \frac{4}{1+u} - \frac{192u}{24(1+u) - \pi^2} \end{aligned} \tag{22}$$

Thus, the first-order Hamiltonian and the zeroth-order eigenfunctions are sufficient to determine the eigenvalue and hence the mass up to the first order in  $\delta$ .

Note that the determination of mass requires us to solve (14) for which we need to perform an integral over all  $Z$ . However, due to normalisability of the eigenfunctions, the integrand contributes insignificantly for large  $Z$ . On the other hand, by taking  $r_c$  small,  $Z$  integration will be dominated by Region I. Thus, we conclude that choosing IR cutoff  $r_c$  arbitrarily small, the meson spectrum can be made independent of Region II and Region III and thus insensitive to UV modes of the gauge theory. Now, of course, we cannot choose  $r_c$  arbitrarily small, since then we need to consider a deformed, resolved cone and our analysis does not apply. However, the normalisability of eigenmodes suggests that even for reasonably large  $r_c$ , the mass computation will be dominated by Region I. This is not surprising since meson physics is a low-energy affair and UV effects can leave the IR intact.

### 3.1.3. Mesons Identification

We would like to verify if this effective model of large  $N$  QCD shares even more similarities with the experiments by comparing the ratios of  $m_n^2$  of well-known vector mesons. In order to do so, we must first identify which kind of mesons are present in this effective theory by looking at their behaviour under charge conjugation ( $\mathcal{C}$ ) and parity ( $\mathcal{P}$ ). The parity operator is a Lorentz transformation flipping the space-like coordinates while charge conjugation corresponds to a flip of the  $Z$  coordinate [13]. Looking at the expansion of the four-dimensional gauge potential (10), we conclude that  $B_\mu^{(n)}$  must be odd (resp. even) under parity/charge conjugation when  $\alpha_n$  is even (resp. odd) in order for  $A_\mu$  to behave as a 4-vector and acquire an overall sign under charge conjugation.



Knowing the eigenvalues of each vector mesons under  $\mathcal{P}$  and  $\mathcal{C}$ , we can identify them using the Particle Data Group (PDG) database [15], where we use their mass measurements  $M_{\text{PDG}}$  for comparison. Also, we concentrate on fields that are vectors of the approximate isospin  $SU(2)$  symmetry as was clarified in [16]. In Table 1, we summarise our knowledge of each of the vector mesons  $B_\mu^{(n)}$  both at the zeroth and first order in  $\delta = g_s M^2/N$ .

**Table 1.** Mass ratio predictions with  $0 < \delta < 0.4$  and a maximal correction of 70%;  $\delta = 0.4000$  and  $u = 0.0528$  minimise  $\chi^2/2$  to 1.4200. The results are compared with both the Sakai–Sugimoto [13] and PDG values [15].

	$\lambda_n/\lambda_m$	Sa-Su	$R_{n/m}^{(0)}$	$R_{n/m}^{(1)}$	$R_{n/m}^{\text{PDG}}$
$m_{a_1(1260)}^2/m_{\rho(770)}^2$	$\lambda_2/\lambda_1$	2.32	2.54	2.34	2.52
$m_{\rho(1450)}^2/m_{\rho(770)}^2$	$\lambda_3/\lambda_1$	4.22	5.27	4.19	3.57
$m_{a_1(1640)}^2/m_{\rho(770)}^2$	$\lambda_4/\lambda_1$	6.62	8.51	6.14	4.51
$m_{\rho(1700)}^2/m_{\rho(770)}^2$	$\lambda_5/\lambda_1$	9.53	12.95	8.46	4.92

Although the results to the first order in  $\delta$  presented in Table 1 are slightly better than the ones of Sakai–Sugimoto [13] and others [17–19], so far the discussions have been confined to the massive KK modes of the *massless* open string sector of the theory. However, open strings also have massive modes, and in principle, these modes can also be identified as mesons. As an example, in Table 1, the  $1^{--}$  states  $\rho(1450)$  and  $\rho(1700)$  could also appear from the massive stringy sector of the model. For the AdS space, an analysis has been performed in [20], where it was shown that the vector meson spectra do get contributions from the massive stringy modes. A similar analysis for our case is rather hard to perform because RR states do not decouple in the simple way as in [20], rendering the quantisation procedure highly non-trivial. This means definite predictions cannot be made at this stage. Thus, for our case, we will continue to use the massless open string sector to study the vector mesons. The other three states appearing in Table 1, namely,  $1^{--}[\rho(770)]$ ,  $1^{++}[a_1(1260)]$  and  $1^{++}[a_1(1640)]$ , are only from the massless open string sector. In addition to that, the massless open string sector cannot be identified with scalar mesons of QCD, since a certain  $Z_2$  symmetry is not shared by the theories, as pointed out in [20]. Thus, our analysis is limited to the study of vector mesons. More details on the scalar meson including its spectrum have appeared in [3].

#### 4. Conclusions

In this note, we have summarised a proposal for a brane configuration and the dual geometry that can mimic several features of large N QCD. For the first time, using a top-down model, where classical description is sufficient, we are able to reproduce some aspects of the RG flow and vector meson spectrum that are consistent with QCD. Our study of normalisable modes on probe branes suggests that vector mesons heavier than the deconfinement scale but lighter than  $\Lambda_0$  (above which the theory is almost CFT) are independent of UV ( $\Lambda > \Lambda_0$ ) physics. By choosing two parameters, we can predict four mass ratios and the results show considerable improvement over previous similar approaches in reaching agreement with experimental data. Although there are many similarities, the brane theory cannot be identified with QCD. The UV is a different, but conformal, theory so is not in the line of an asymptotically free theory. Additionally, the massive string modes start contributing at this energy scale and change the masses of the vector mesons. Such changes could, in principle, improve the analysis presented here but are harder to study because of technical challenges. In [21–23], new progress has been made which further elaborates

on the analysis presented here. In fact, refs [21–23] have been able to argue how the holographic model presented here and in [24] can resolve many subtle issues associated with mesonic interactions in large  $N$  QCD. The interference from the massive modes appears to not change the result in any significant way, although more work needs to be done to confirm what happens when going to very heavy mesonic modes. Therefore to conclude, the holographic techniques presented here should be best utilised as tools to gain analytic understanding of the non-perturbative regimes of QCD.

**Author Contributions:** Conceptualization, M.M., K.D., C.G. and O.T.; Methodology, M.R. All authors have read and agreed to the published version of the manuscript.

**Funding:** Natural Sciences and Engineering Research Council of Canada (NSERC), Grant Number 210381; and Department of Energy (DOE), Grant Number DE-SC0007884.

**Data Availability Statement:** The original contributions presented in this study are included in the article.

**Acknowledgments:** It is a great pleasure to thank Shigeki Sugimoto, Peter Ouyang and Martin Kruczenski for helpful discussions.

**Conflicts of Interest:** The authors declare no conflicts of interest.

## References

- Maldacena, J.M. The Large  $N$  Limit of Superconformal Field Theories and Supergravity. *Adv. Theor. Math. Phys.* **1998**, *2*, 231–252. [[CrossRef](#)]
- Klebanov, I.R.; Strassler, M.J. Supergravity and a Confining Gauge Theory: Duality Cascades and  $\chi$ SB-Resolution of Naked Singularities. *J. High Energy Phys.* **2000**, *2000*, 052. [[CrossRef](#)]
- Dasgupta, K.; Gale, C.; Mia, M.; Richard, M.; Trottier, O. Infrared Dynamics of Large  $N$  QCD, Massless Stringy Sector, and Mesonic Spectra. *J. High Energy Phys.* **2015**, *2015*, 122. [[CrossRef](#)]
- Klebanov, I.R.; Witten, E. Superconformal field theory on three-branes at a Calabi-Yau singularity. *Nucl. Phys. B* **1998**, *536*, 199–218. [[CrossRef](#)]
- Mia, M. Thermodynamics of large  $N$  gauge theory from top down holography. *Phys. Rev. D* **2014**, *89*, 043010. [[CrossRef](#)]
- Mia, M.; Dasgupta, K.; Gale, C.; Jeon, S. Five Easy Pieces: The Dynamics of Quarks in Strongly Coupled Plasmas. *Nucl. Phys. B* **2010**, *839*, 187–293. [[CrossRef](#)]
- Mia, M.; Dasgupta, K.; Gale, C.; Jeon, S. Toward Large  $N$  Thermal QCD from Dual Gravity: The Heavy Quarkonium Potential. *Phys. Rev. D* **2010**, *82*, 026004. [[CrossRef](#)]
- Mia, M.; Chen, F.; Dasgupta, K.; Franche, P.; Vaidya, S. Non-Extremality, Chemical Potential and the Infrared limit of Large  $N$  Thermal QCD. *Phys. Rev. D* **2012**, *86*, 086002. [[CrossRef](#)]
- Hawking, S.W.; Page, D.N. Thermodynamics Of Black Holes In Anti-De Sitter Space. *Commun. Math. Phys.* **1983**, *87*, 577. [[CrossRef](#)]
- Witten, E. Anti-de Sitter space, thermal phase transition, and confinement in gauge theories. *Adv. Theor. Math. Phys.* **1998**, *2*, 505–532. [[CrossRef](#)]
- Mia, M.; Chen, F. Non extremal geometries and holographic phase transitions. *J. High Energy Phys.* **2013**, *2013*, 83. [[CrossRef](#)]
- Kuperstein, S. Meson spectroscopy from holomorphic probes on the warped deformed conifold. *J. High Energy Phys.* **2005**, *2005*, 014. [[CrossRef](#)]
- Sakai, T.; Sugimoto, S. Low energy hadron physics in holographic QCD. *Prog. Theor. Phys.* **2005**, *113*, 843–882. [[CrossRef](#)]
- Sakai, T.; Sugimoto, S. More on a holographic dual of QCD. *Prog. Theor. Phys.* **2005**, *114*, 1083–1118. [[CrossRef](#)]
- Berenger, J. Particle Data Group Collaboration. Review of particle physics. Particle Data Group. *Phys. Rev. D* **2012**, *86*, 010001.
- Son, D.T.; Stephanov, M.A. QCD and dimensional deconstruction. *Phys. Rev. D* **2004**, *69*, 065020. [[CrossRef](#)]
- Kruczenski, M.; Mateos, D.; Myers, R.C.; Winters, D.J. Meson spectroscopy in AdS / CFT with flavor. *J. High Energy Phys.* **2003**, *2003*, 049. [[CrossRef](#)]
- Ihl, M.; Torres, M.A.C.; Boschi-Filho, H.; Bayona, C.A.B. Scalar and vector mesons of flavor chiral symmetry breaking in the Klebanov-Strassler background. *J. High Energy Phys.* **2011**, *2011*, 026. [[CrossRef](#)]
- Cotrone, A.L.; Dymarsky, A.; Kuperstein, S. On Vector Meson Masses in a Holographic SQCD. *J. High Energy Phys.* **2011**, *2011*, 005. [[CrossRef](#)]

20. Imoto, T.; Sakai, T.; Sugimoto, S. Mesons as Open Strings in a Holographic Dual of QCD. *Prog. Theor. Phys.* **2010**, *124*, 263–284. [[CrossRef](#)]
21. Yadav, V.; Misra, A. M-Theory Exotic Scalar Glueball Decays to Mesons at Finite Coupling. *J. High Energy Phys.* **2018**, *2018*, 133. [[CrossRef](#)]
22. Sil, K.; Yadav, V.; Misra, A. Top-down holographic G-structure glueball spectroscopy at (N)LO in  $N$  and finite coupling. *Eur. Phys. J. C* **2017**, *77*, 381. [[CrossRef](#)]
23. Misra, A.; Yadav, G. QCD-compatible supermassive inert top-down holographic mesinos at intermediate coupling. *Phys. Rev. D* **2023**, *108*, 106013. [[CrossRef](#)]
24. Dhuria, M.; Misra, A. Towards MQGP. *J. High Energy Phys.* **2013**, *2013*, 1. [[CrossRef](#)]

**Disclaimer/Publisher's Note:** The statements, opinions and data contained in all publications are solely those of the individual author(s) and contributor(s) and not of MDPI and/or the editor(s). MDPI and/or the editor(s) disclaim responsibility for any injury to people or property resulting from any ideas, methods, instructions or products referred to in the content.